Revista Brasileira de Ensino de Física, vol. 45, e20230217 (2023)
www.scielo.br/rbef
DOI: https://doi.org/10.1590/1806-9126-RBEF-2023-0217

Enhancing learning of the Grad-Shafranov equation through scientific literature: part 2 of a physics education series

L. Nunes dos Santos[1,2], A. Ojeda-González[*1], V. De La Luz[3], V. Klausner[1], S. Pilling[1], A. Prestes[1], A. N. Laurindo Sousa[4], M. Cristaldo-Oliveira[1,5]

[1]Universidade do Vale do Paraíba, Instituto de Física e Astronomia, São José dos Campos, SP, Brasil.
[2]Universidade Federal de Mato Grosso do Sul, Departamento de Matemática, Aquidauana, MS, Brasil.
[3]Universidad Nacional Autónoma de México, Unidad Morelia, Escuela Nacional de Estudios Superiores, Morelia, Michoacán, Mexico.
[4]Universidade Estadual do Maranhão, Centro de Estudos Superiores de Balsas, Departamento de Matemática, Balsas, MA, Brasil.
[5]Superintendência de Politicas Educacionais, Secretaria de Estado de Educação de Mato Grosso do Sul, Campo Grande, MS, Brasil.

Received on August 08, 2023. Accepted on October 03, 2023.

In part 1 of our physics education series, we introduced a novel solution based on Yoon-Lui's solutions 1 and 2. Building upon that, this follow-up presents a new solution obtained by combining the generating functions of Yoon-Lui-1 and Yoon-Lui-3, resulting in a new and simplified general solution. We also calculate the singular points and determine their coordinates for various parameter values. A graphical representation of the solution is presented, showing the magnetic field lines and current density distribution. The behavior of the magnetic field and the effect of varying the parameter are discussed. The observed magnetic islands and singular points are relevant in the fields of Plasma Physics and Space Physics, providing insights into magnetic structures in plasmas and their impact on confinement and stability. Furthermore, this study encourages innovation and equips researchers and students with the necessary tools to make meaningful contributions to the field, emphasizing the integration of scientific literature into physics education to promote a comprehensive understanding of physical concepts and their practical applications.
Keywords: Grad-Shafranov equation, Magnetic flux-ropes, Plasma confinement, Singularity analysis.

1. Introduction

The scientific method is crucial to understanding the physical world around us. As scientists, we observe recurring phenomena and propose explanations based on our existing knowledge, testing and refining these explanations through experiments and research. In physics education, it is essential to teach students how to use scientific literature to create new ideas and innovations, fostering a deeper understanding of physical concepts and their applications. Within this context, part 1 of our physics education series [1] introduced a novel solution based on Yoon-Lui's solutions 1 and 2. In this continuation of our series, we present another new solution to the specific Grad-Shafranov (GS) equation by combining two generating functions proposed by Yoon and Lui (2005), the Yoon-Lui-1 and Yoon-Lui-3 solutions. This new solution may offer greater plasma confinement efficiency and specific mathematical methods such as combining generating functions were used to obtain it.

The hypothesis of the new solution will be presented, and its validity will be evaluated in later sections of this article. By applying the findings and techniques from Yoon and Lui's work, we aim to inspire and empower the next generation of physicists with the knowledge and tools needed to make meaningful contributions to the field.

One illustrative example of how scientific knowledge can be used to gain insights into complex systems is the GS equation, a fundamental tool in plasma physics with a wide range of applications in Space Physics, such as magnetic reconnection, plasma turbulence, and flux tubes in planetary magnetospheres, and magnetic confinement in tokamaks [2–5].

The GS equation has also led to the development of the Grad-Shafranov reconstruction (GSR) technique, which is particularly useful for reconstructing magnetic field topology in regions of plasma and has been applied to structures of plasma in the geospace, such as current sheets in the magnetopause and associated structures, and multiple flux tubes from interplanetary coronal mass ejections [6–12]. Additionally, the GS equation has been

*Correspondence email address: arian@univap.br

used to develop new analytical solutions, which have been used to model complex plasma dynamics in the geospace and have helped to further our understanding of plasma physics [13–21].

This article is organized into six sections. In Section 2, we discuss in detail the GS equation, whose importance in plasma physics was previously addressed during the introduction. In Section 3, we review the analytical solution proposed by Yoon and Lui in 2005, with an emphasis on the characteristics of the Yoon-Lui-3 solution. We also address the solution presented in Part 1 of this article and its characteristics in Section 3.2.

In Section 4, we describe the methodology used to obtain the new solution, which combines the features of the Yoon-Lui-1 and Yoon-Lui-3 solutions. In Section 5, we present the results obtained and analyze the effectiveness of the new solution. In addition, we discuss the implications of the results obtained and how the new solution can contribute to the understanding of plasma physics. Finally, in Section 6, we conclude the article by highlighting the main contributions of this work and the possible directions for future research in this area. The third part of this research will present another new solution, which will be described in a separate article. This solution was also obtained from the solutions of Yoon and Lui (2005).

2. Specific Grad-Shafranov equation

The GS equation is a significant partial differential equation in physics [22, 23]. It can be expressed as follows:

$$\frac{\partial^2 A_y(x,z)}{\partial x^2} + \frac{\partial^2 A_y(x,z)}{\partial z^2} = -\mu_0 \frac{d}{dA_y}\left(P_t(A_y(x,z))\right). \tag{1}$$

Here, A_y represents the y-component of the magnetic vector potential. On the left-hand side, it is defined as the Laplacian of the magnetic potential vector (A), while the right-hand side represents the current density, which is a function of the first derivative of pressure with respect to A [8, 24].

It is worth noting that this type of partial differential equation lacks an analytical solution and is commonly solved numerically as a Cauchy problem. However, when considering the current density as an exponential function of the magnetic potential vector, the equation acquires an analytical solution and is commonly referred to as the specific GS equation [7, 25–27].

It is important to validate a proposed numerical solution by comparing it with an analytical solution [27]. To achieve this, simplifications can be made to the equation that allow the elimination of non-linearity [28]. In this way, a general analytical solution can be obtained that meets the initial conditions for implementing the numerical solution. We explained the step-by-step procedure to obtain an analytical solution to the equation in the previous article, which we refer to as Part 1 [1]. The term on the right-hand side of the equation (1) defines the plasma transverse pressure, which is used to obtain an analytical solution for specific cases.

The specific form of the GS equation used in the current work is given by

$$\frac{\partial^2 \Psi(X,Z)}{\partial X^2} + \frac{\partial^2 \Psi(X,Z)}{\partial Z^2} = e^{-2\Psi(X,Z)}, \tag{2}$$

considering new dimensionless variables: $\frac{x}{L} = X$, $\frac{z}{L} = Z$, and $\Psi(X,Z) = -\frac{A_y}{LB_0}$ is the normalized magnetic vector potential, where B_0 is the asymptotic magnetic field, L represents the scale length [29]. It is worth noting that (2) is a Poisson-like equation with a non-homogeneous term that takes an exponential form. Additionally, the 'Walker formula' [30] proposed in 1915 is introduced as follows:

$$e^{-2\Psi(X,Z)} = \frac{4|g(\zeta)'|^2}{\left(1+|g(\zeta)|^2\right)^2}. \tag{3}$$

Equation (3) is a general solution to Equation (2) that depends on a complex analytic function called the generating function, $g(\zeta)$ where ζ is a complex variable. The Walker formula has been utilized for proposing new analytical solutions to the GS equation, and further discussion on this will be provided in the next section. It is worth noting that the GS equation was derived by Kan in 1973 from Plasma Kinetic Theory by solving the set of Vlasov-Maxwell equations. For more details on the physical-theoretical formulation of the GS equation using Kinetic Theory, we refer the reader to [25, 28].

3. Review of the analytical solution

This section aims to demonstrate the contribution of studying scientific literature in acquiring new knowledge related to the GS equation. To illustrate this point, reference will be made to Yoon and Lui's work (2005), which provides analytical solutions for the GS equation based on the Walker formula presented in equation (3). In a previous publication [1], nine solutions presented by the authors were described. However, for the purpose of this part 2 article, the focus will exclusively be on the three solutions proposed by Yoon and Lui. These solutions will serve as the foundation for the study and are outlined below:

1. Yoon-Lui-1 solution [31, sections 3.7], which has the form:

$$g(\zeta) = \zeta^{\nu}, \tag{4}$$

and

$$\Psi(X,Z) = ln\frac{R(R^{\nu}+R^{-\nu})}{2\nu}. \tag{5}$$

In this solution, $R^2 = X^2 + Z^2$, where X and Z are variables in the Cartesian plane, and ν is a parameter that can affect the morphology of the solution.

2. Yoon-Lui-2 solution [31, section 3.8] is given by

$$g(\zeta) = \zeta - \frac{a}{\zeta}, \tag{6}$$

and

$$\Psi(X, Z) = ln\frac{(R^2 + a)^2 + R^2 - 4aX^2}{2[(R^2 + a)^2 - 4aZ^2]^{1/2}}. \tag{7}$$

3. Yoon-Lui-3 solution [31, section 3.9] is given by

$$g(\zeta) = \frac{\zeta}{(1 - a^2\zeta^2)}, \tag{8}$$

and

$$\Psi(X, Z) = \frac{1}{2}\ln(\frac{S(S + R^2)^2}{2T}), \tag{9}$$

where $S = (1-a^2R^2)^2+(2aZ)^2$, $T = (1-a^4R^4)^2+(4a^2XZ)^2$, and a is a parameter that can affect the morphology of the solution.

We will propose new solutions derived from solutions refer to as Yoon-Lui-1 and Yoon-Lui-3. It is important to note that all of these solutions were obtained from the Walker formula presented in Equation (3). In the following section, more details about the Yoon-Lui-1 and Yoon-Lui-3 solutions will be presented, followed by a discussion of the solution reported by us in the previous article (Part 1).

3.1. An In-Depth Look at Yoon-Lui-1 and Yoon-Lui-3 Solutions

The Yoon-Lui-1 solution (5) is an exact analytical solution of the specific GS equation for a magnetic island-type configuration. It has a single singularity when $\nu \neq 1$ at the point $(0, 0)$ and maximum current density at the center of the magnetic island. The solution is expressed in terms of elementary functions and is useful for validating numerical solutions and analyzing the stability of magnetic structures. It is recommended to use $\nu = 1$ when applying the solution to the analysis of a magnetic flux rope with magnetic island configuration, as there are no singularities in the solution. In the first article of this series (Part 1), a graph of the solution in question was presented and its peculiar characteristics were discussed. For readers interested in gaining a better understanding of this solution, it is recommended to read the first part of the series.

Henceforth, the details of the Yoon-Lui-3 solution, introduced in Equation (9), will be presented. Moving forward, an analysis of its singularities will be conducted, along with the corresponding graph.

Before delving into the analysis of the equation´s singularities, establishing a mathematical context is crucial. To accomplish this, the focus will be on solutions obtained from the Walker formula, and the singularities of $\Psi(X, Z)$ will be explored. Traditionally, examining the function Ψ was used to locate the singularities, which could be complicated. However, [32] introduced a more straightforward approach using the generating function $g(\zeta)$, which must satisfy the condition

$$\nabla \ln |g'(\zeta)| = 0. \tag{10}$$

By rewriting equation (3) and applying the *nabla* operator to

$$\Psi(\zeta) = -\frac{1}{2}\ln\left(\frac{4\,|g'(\zeta)|^2}{(1 + |g(\zeta)|^2)^2}\right), \tag{11}$$

we obtain

$$\begin{aligned}\nabla\Psi(\zeta) &= -\nabla \ln |g'(\zeta)| + \nabla \ln\left(1 + |g(\zeta)|^2\right)\\ &= -\nabla \ln |g'(\zeta)| + \frac{4\,|g(\zeta)'|^2}{(1 + |g(\zeta)|^2)^2},\end{aligned} \tag{12}$$

which is equal to (3) if $\nabla \ln |g'(\zeta)| = 0$. Therefore, to locate singularities, we must calculate $|g'(\zeta)| = 0$. This allows us to determine the singular points (X, Z) of $\Psi(X, Z)$ directly from $g'(\zeta)$, as well as from $\Psi(X, Z)$ itself.

We will begin by taking the derivative of the generating function given in (8). Consider

$$g'(\zeta) = \frac{1 + a^2\zeta^2}{(1 - a^2\zeta^2)^2}. \tag{13}$$

By evaluating the modulus of the function in (13), we obtain

$$|g'(\zeta)| = \left(\frac{1 + a^2\zeta^2}{(1 - a^2\zeta^2)^2}\right)^{\frac{1}{2}} \cdot \left(\frac{1 + a^2\zeta^{*2}}{(1 - a^2\zeta^{*2})^2}\right)^{\frac{1}{2}} = X_1. \tag{14}$$

Now, let's calculate $\nabla \ln |g'(\zeta)| = 0$ as follows

$$\begin{aligned}&\nabla \ln X_1\\ &\quad= \frac{1}{2}\nabla\left[\ln\left(\frac{1 + a^2\zeta^2}{(1 - a^2\zeta^2)^2}\right) + \ln\left(\frac{1 + a^2\zeta^{*2}}{(1 - a^2\zeta^{*2})^2}\right)\right]\\ &\quad= 2\frac{\partial}{\partial\zeta}\left(\frac{\partial}{\partial\zeta^*}\left[\ln\left(\frac{1 + a^2\zeta^2}{(1 - a^2\zeta^2)^2}\right) + \ln\left(\frac{1 + a^2\zeta^{*2}}{(1 - a^2\zeta^{*2})^2}\right)\right]\right)\\ &\quad= 2\frac{\partial}{\partial\zeta}\left(\frac{2a^2\zeta^*[3 - a^2\zeta^{*2}]}{1 - a^4\zeta^{*4}}\right)\\ &\quad= 4 \cdot 0 = 0.\end{aligned} \tag{15}$$

From (15), we have the first condition satisfied. Now we will calculate the singularities, substituting $\zeta = X + iZ$ into equation (14), as follows

$$\begin{aligned}X_1 = &\left(\frac{1 + a^2(X + iZ)^2}{(1 - a^2(X + iZ)^2)^2}\right)^{\frac{1}{2}}\\ &\times\left(\frac{1 + a^2(X - iZ)^2}{(1 - a^2(X - iZ)^2)^2}\right)^{\frac{1}{2}} = 0.\end{aligned} \tag{16}$$

In (16), the identity only occurs when $(1 - a^2(X + iZ)^2)^2 = 0$ or $(1 - a^2(X - iZ)^2)^2 = 0$. Therefore, for both cases, we have the following singularities set: $\left(0, \pm\frac{1}{a}\right)$.

Note that when $a = 0.7$ we have two singularities on the Z axis, precisely at the points $\left(0, \pm\frac{1}{|a|}\right)$, which in numerical values are $(0, \pm 1.429)$, as we can see in Figure 1.

Figure 1 consists of four panels showing the graph of the equation named in (9), which is the solution of the Yoon-Lui-3 model as a function of the normalized magnetic vector potential (Ψ). To construct the graph, a density plot was used by projecting the magnetic field onto the XZ cartesian plane, allowing for visualization of the vector field. The magnetic field is calculated from Ψ and overlaid on the same graph with the normalized current density J_y, ranging from 0 to 1, using a color palette beginning with dark blue, ranging through shades of blue, cyan, green, yellow and red, and ending with dark red.

The solution 9 depends on the parameter a, which is of vital importance because it allows changing the configuration of the magnetic field projection. The solution exhibits two singular points at $\left(0, \pm\frac{1}{|a|}\right)$, whose location is above the Z cartesian axis and depends on the value of the parameter a, which is always positive.

It is worth noting that, for very high values of a (for example, $a = 18$), when analyzing the graph on the scale shown in Figure 1, the structure of magnetic islands is lost because both the islands and the singular points attempt to converge towards the origin. When the value of a is very small, the singularities move significantly away from the origin, as observed in panel a) of Figure 1. At this scale, a magnetic island at the point $(0, 0)$ is visually noticeable, very similar to the case of the Yoon-Lui-1 solution when $\nu = 1$. Therefore, it's worth pointing out that at a smaller scale, there are differences in the current density values at the origin of the coordinate system for both solutions. In the case of the Yoon-Lui-1 solution when $\nu = 1$, the current density reaches its maximum value at the point (0,0). In the case of the Yoon-Lui-3 solution with $a = 0.1$, the current density does not reach its maximum at the point $(0, 0)$ but instead has two maxima symmetrically located close to the origin, above the X-axis.

A phenomenon that makes the Yoon-Lui-3 solution very interesting is that by increasing the value of a, both singular points are brought to the origin, form an X-point between two magnetic islands. This phenomenon, known in plasma physics as coalescence [33, 34], forms a neutral X-type point at the origin. This configuration obtained in this analytical solution can be useful for studying certain aspects of plasma behavior. To further clarify, coalescence is a phenomenon in which two or more magnetic vortices in a plasma come closer together and merge into a single structure. Coalescence is a crucial phenomenon as it can impact both plasma stability and the efficacy of nuclear fusion.

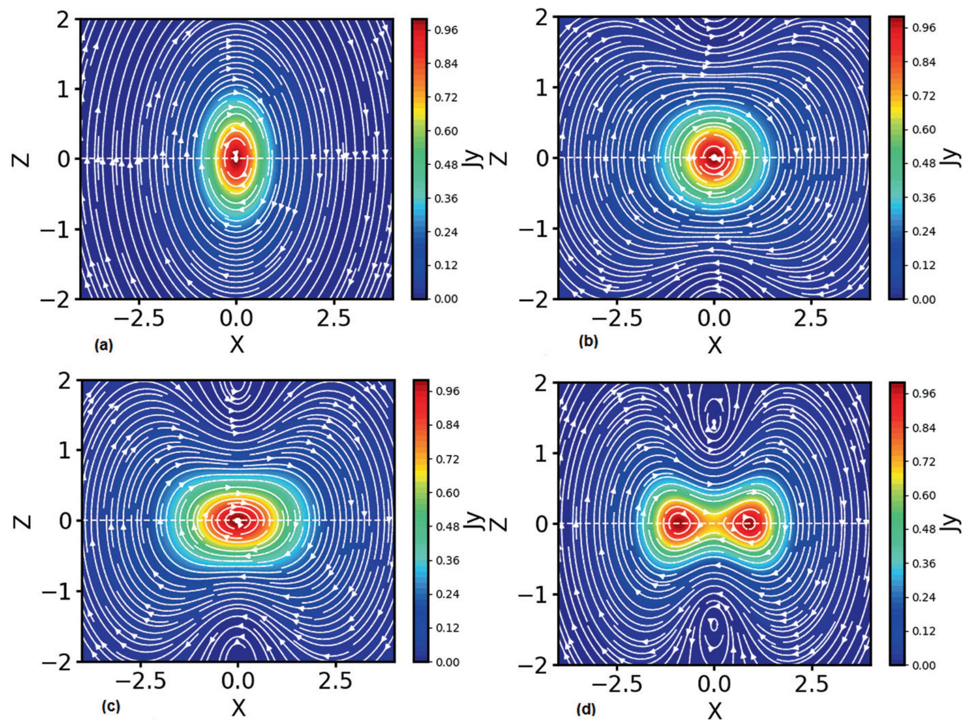

Figure 1: The density plot of the Yoon-Lui-3 solution, defined by equation (9), displays four panels that illustrate different conditions with parameters $a = 0.1$, 0.4, 0.5, and 0.7. Each panel shows the magnetic island and the singularities, allowing for the observation of changes as a increases from 0.1 (panel a) to 0.7 (panel d). It is worth noting that in panel d), the coalescence of the islands can be observed, with the formation of the X-point.

Specifically, in tokamaks, which are devices employed for plasma confinement in a ring shape, coalescence may result in a plasma confinement loss and thus a reduction in fusion efficacy [35]. Moreover, coalescence is a fundamental phenomenon for comprehending the evolution of intricate magnetic systems in general, such as the Earth's magnetosphere and solar winds [36]. The investigation of coalescence in plasmas enables us to gain a better understanding of the magnetic systems' dynamics.

After all the previous explanations, it is important to inform the reader that Figure 1 shows the entire phenomenon described so far. The four panels were represented on a grid from -3 to 3 on the X-axis and from -2 to 2 on the Z-axis. In panel a), we have the case $a = 0.1$, and the magnetic island appears isolated at the origin, without the presence of singularities. In panel b), we have $a = 0.4$, and both singularities begin to appear along the edges above the Z-axis, but the magnetic island continues to appear isolated at the origin, with some changes in geometry when compared to panel a). In panel c), $a = 0.5$ was considered, and the singular points are much closer to the origin, which disrupts the island, which still appears isolated but much more elongated in an elliptical shape above the X-axis. Finally, in panel d), we have $a = 0.7$, and it is possible to clearly observe the division of the islands, *i.e.*, the coalescence, with the formation of the X-point between them.

3.2. Details of the solution obtained in part 1 article

In [1], a novel solution for GS equation was presented, obtained through a specific mathematical approach that involves combining the generating functions of the Yoon-Lui-1 and Yoon-Lui-2 models

$$g(\zeta) = \frac{\zeta^\nu}{\frac{\zeta^2 - a}{\zeta}} = \frac{\zeta^{\nu+1}}{\zeta^2 - a}, \tag{17}$$

where ν and a are constants. The resulting generating function is then substituted into the Walker formula to obtain the final solution, which is given by

$$\Psi(X, Z) = \ln\left[\frac{R^{2(\nu+1)} + a^2 - 2aT^2 + R^4}{2\sqrt{R^{2\nu}\left[\left[(\nu-1)T^2 - a(\nu+1)\right]^2 + (\nu-1)^2U^2\right]}}\right]. \tag{18}$$

Three parameters are introduced, namely

$$R^2 = X^2 + Z^2, \tag{19}$$

$$U^2 = 4X^2Z^2, \tag{20}$$

$$T^2 = X^2 - Z^2. \tag{21}$$

The proposed solution, shown in Figure 2, exhibits singularities at specific points in the domain, which

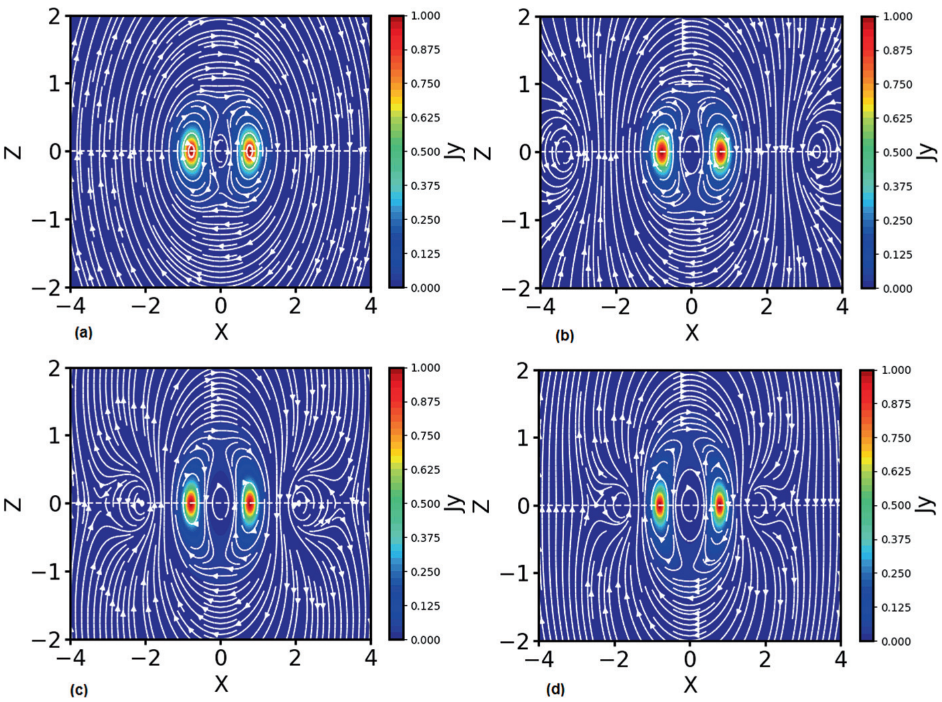

Figure 2: The density plot above shows the proposed solution given by equation (18) from [1]. The figures in each panel were generated by keeping the value of a fixed at 1 and varied ν in each of the four images: $\nu = 1.0$, $\nu = 1.2$, $\nu = 1.6$, and $\nu = 2.0$, respectively labeled *a)* to *d)*. The singular points, which are located at the points $(0, 0)$, $(\pm\sqrt{11}, 0)$, $\left(\pm\sqrt{\frac{13}{3}}, 0\right)$, and $\left(\pm\sqrt{3}, 0\right)$ for each value of ν, are indicated in each image. These points are crucial for analyzing the behavior of the proposed solution in specific regions of the domain and for understanding the solution's behavior in different regimes.

are associated with the physical characteristics of the solution. These singular points are crucial for analyzing the solution's behavior in specific regions of the domain and understanding its behavior in different regimes. The solution may contribute to improving plasma confinement efficiency in confined plasma regions. As ν increases, the singular points move closer to the magnetic islands, resulting in more effective confinement. This solution has potential for applications in confined plasma systems, with potential benefits for plasma confinement efficiency.

4. Methodology

This work presents a new solution for the magnetic field in a confined plasma system, obtained by combining the Yoon-Lui-1 and Yoon-Lui-3 generating functions through a mathematical transformation.

The process begins with the development of the mathematical derivation until the new generating function is obtained. Subsequently, the generating function is substituted into the Walker formula presented in (3), and algebraic calculations are performed to obtain the expression for $\Psi(X, Z)$. The proposed solution is analyzed using the Génot criterion to examine the singular points.

In summary, density graphs are generated for various values of the parameter ν to assess the behavior of the proposed solution. These graphs enable the verification of the singular points, which play a crucial role in understanding the magnetic field and current density behavior across different regions of the domain. Furthermore, the potential applications of the proposed solution and its contribution to enhancing plasma confinement efficiency are discussed.

Ultimately, we observe that the methodology presented in this work combines mathematical analysis with physical interpretation to derive and analyze a novel solution for the magnetic field in a confined plasma system. The integrated approach of this study contributes to advancing our understanding of plasma physics and holds promise for practical applications in plasma confinement.

5. Results and Discussion

The solution obtained combines the generating functions of Yoon-Lui-1 and Yoon-Lui-3 by means of their quotient. The calculations lead to the following generating function

$$g(\zeta) = \frac{\zeta^{\nu}}{\frac{\zeta}{1-a^2\zeta^2}} = \zeta^{\nu-1} - a^2\zeta^{\nu+1}, \tag{22}$$

where ν and a are constants.

By substituting $\zeta = X + iZ$ and calculating the square of the modulus of $g(\zeta)$, we obtain

$$|g(\zeta)|^2 = (X^2+Z^2)^{\nu-1} \times \left[a^4\left(X^2+Z^2\right)^2 - 2a^2\left(X^2-Z^2\right)+1\right]. \tag{23}$$

Adding 1 to both sides of the previous equation, we have

$$1+|g(\zeta)|^2 = 1+(X^2+Z^2)^{\nu-1} \times \left(a^4\left(X^2+Z^2\right)^2 - 2a^2\left(X^2-Z^2\right)+1\right). \tag{24}$$

Continuing with the reasoning, the first derivative of the generating function is

$$g'(\zeta) = \zeta^{\nu-2}\left[(\nu-1) - a^2(\nu+1)\zeta^2\right], \tag{25}$$

and its modulus is

$$|g'(\zeta)| = \sqrt{(X^2+Z^2)^{\nu-2}} \times \sqrt{\Big[((\nu-1) - a^2(\nu+1)(X-iZ)^2)} \times \sqrt{((\nu-1) - a^2(\nu+1)(X+iZ)^2)\Big]}. \tag{26}$$

After some algebraic manipulations, we can eliminate the imaginary unit from the module of the derivative of the generating function

$$|g'(\zeta)| = \sqrt{(X^2+Z^2)^{\nu-2}} \times \sqrt{\left[((\nu-1) - a^2(\nu+1)(X^2-Z^2))^2 + 4a^4(\nu+1)^2X^2Z^2\right]}. \tag{27}$$

Finally, by substituting (24) and (27) in *Walker*'s formula (3), and using the three parameters presented in (19), (20) and (21), the equation is simplified and the resulting expression is

$$\Psi(X, Z) = \ln\left[\frac{1+R^{2(\nu-1)}\left(a^4R^4 - 2a^2T^2+1\right)}{2\sqrt{R^{2(\nu-2)}}\times} \times \frac{1}{\sqrt{\left[\left((\nu-1) - a^2(\nu+1)T^2\right)^2 + 4a^4(\nu+1)^2U^2\right]}}\right]. \tag{28}$$

From this point on, we will proceed to calculate the singular points of the solution (28). We begin by obtaining the derivative of the generating function, $g(\zeta) = \zeta^{\nu-1} - a^2\zeta^{\nu+1}$, as

$$g'(\zeta) = (\nu-1)\zeta^{\nu-2} - a^2(\nu+1)\zeta^{\nu}, \tag{29}$$

from which we calculate the modulus

$$|g'(\zeta)| = \sqrt{[(\nu-1)\zeta^{\nu-2} - a^2(\nu+1)\zeta^{\nu}]} \times \sqrt{[(\nu-1)\zeta^{*\nu-2} - a^2(\nu+1)\zeta^{*\nu}]}. \quad (30)$$

Expanding the equation $\nabla \ln |g'(\zeta)| = 0$, we have

$$\nabla \ln |g'(\zeta)| = 4\frac{\partial}{\partial \zeta}\left(\frac{\partial}{\partial \zeta^*}\ln\left((\nu-1)\zeta^{\nu-2} - a^2(\nu+1)\zeta^{\nu}\right)^{\frac{1}{2}} \times \ln\left((\nu-1)\zeta^{*\nu-2} - a^2(\nu+1)\zeta^{*\nu}\right)^{\frac{1}{2}}\right).$$

Continuing with the development, we have

$$\begin{aligned}\nabla \ln |g'(\zeta)| &= 4\frac{\partial}{\partial \zeta}\left(\frac{(\nu-1)(\nu-2) - a^2\nu\zeta^{*2}(\nu+1)}{2\zeta^*(\nu - a^2\zeta^{*2}(\nu+1) - 1)}\right), \\ &= 4 \cdot 0, \\ &= 0. \end{aligned} \quad (31)$$

By (31), we have the first condition satisfied. Now we will look for the singularities. Substituting (30), we get

$$\sqrt{[(\nu-1)\zeta^{\nu-2} - a^2(\nu+1)\zeta^{\nu}]} \times \sqrt{[(\nu-1)\zeta^{*\nu-2} - a^2(\nu+1)\zeta^{*\nu}]} = 0. \quad (32)$$

After some algebraic manipulations, equation (32) will be valid if, and only if

$$[(\nu-1)(X+iZ)^{\nu-2} - a^2(\nu+1)(X+iZ)^{\nu}] \times [(\nu-1)(X-iZ)^{\nu-2} - a^2(\nu+1)(X-iZ)^{\nu}] = 0. \quad (33)$$

Therefore, $(\nu-1)(X+iZ)^{\nu-2} - a^2(\nu+1)(X+iZ)^{\nu} = 0$ or $(\nu-1)(X-iZ)^{\nu-2} - a^2(\nu+1)(X-iZ)^{\nu} = 0$, notice that there is a variable in the exponent. Thus, to understand, we can look at some cases. For example, if $a = 1$ and $\nu = 1$, we would have

$$-2(X+iZ)^1 = 0, \quad (34)$$

whose only solution would be $(0, 0)$.

Now, for any $\nu \neq -1$ and $a \neq 0$, we would have the following solution for the singularities

$$\zeta = \zeta^* = \pm\sqrt{\frac{\nu-1}{a^2(\nu+1)}}, \quad (35)$$

that is, the singular points are: $\left(\pm\sqrt{\frac{\nu-1}{a^2(\nu+1)}}, 0\right)$.

Now, fixing $a = 1$ and varying the value of ν, we have the following singular points

- $\nu = 1$; $\zeta = (0, 0)$;
- $\nu = 1.6$; $\zeta = (\pm 0.48, 0)$;
- $\nu = 1.8$; $\zeta = (\pm 0.53, 0)$;
- $\nu = 2$; $\zeta = (\pm 0.58, 0)$;
- $\nu = 3$; $\zeta = (\pm 0.71, 0)$;
- $\nu = 4$; $\zeta = (\pm 0.77, 0)$.

Figure 3 comprises six panels displaying the graph of the equation named in (28), which is the solution we propose in this manuscript as a function of the normalized magnetic vector potential (Ψ). To construct the graph, a density plot was used, projecting the magnetic field onto the XZ Cartesian plane, allowing the visualization of the vector field. The magnetic field is calculated from Ψ and overlaid on the same graph with the normalized current density J_y, ranging from 0 to 1, using a color palette. We fixed the value of $a = 1$ and varied the parameter ν with the follows values: 1.0, 1.6, 1.8, 2.0, 3.0, and 4.0, representing the graphs in panels a) to f), respectively. The six panels are represented on a grid from -2 to 2 on the X-axis and from -1 to 1 on the Z-axis. The singularity points are located at: $(0, 0)$, $(\pm 0.48, 0)$, $(\pm 0.53, 0)$, $(\pm 0.58, 0)$, $(\pm 0.71, 0)$, $(\pm 0.77, 0)$, in panels a) to f), respectively.

The six panels in this figure illustrate the behavior of the magnetic field generated by the electrical current distribution described by the solution presented in (28). The panels reveal how the magnetic field lines curve and change direction in response to the current distribution, and also depict regions of varying magnetic field intensities. The panels also display the locations of singularities in the solution, where the magnetic field becomes infinite, and the effect of varying the parameter ν on the shape of the magnetic field.

Taking a closer look at the panels in Figure 3, interesting details can be observed. In panel a), there is a single singular point at the origin, easily detectable in the figure due to the counterclockwise orientation of the magnetic field. The two magnetic islands are well-defined and symmetrically positioned above the X-axis. Additionally, neutral X-points appear above the Z-axis at the interface between the external field surrounding the structures, the field encircling each island, and the field enveloping the singular point, respectively. This structure is similar to the one presented in the solution by [37], with the difference that the structures are non-periodic. This behavior also resembles Figure 2a, corresponding to the solution proposed in our initial article, where we stated that this stable configuration could be advantageous for confining plasma within the magnetic islands.

In panel b), the field morphology undergoes an abrupt change. Maintaining $a = 1$ but with $\nu = 1.6$, two equally spaced singular points appear above the X-axis while the singular point at the origin remains. Observing this process as a dynamic continuity from panel a), it is as if there were a coalescence of the singular point, and the islands are displaced further away from the Z-axis, equidistant from each other. In this initial stage of the process, no current density accumulation is observed in

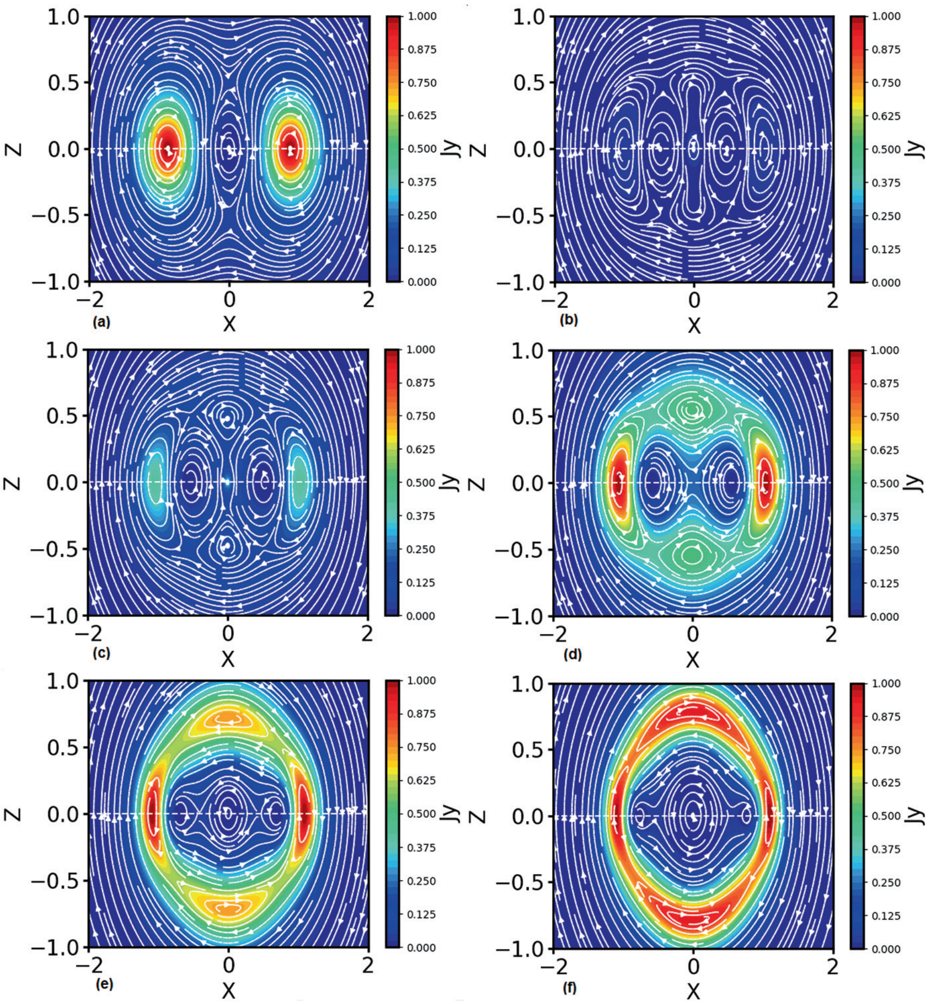

Figure 3: This figure displays the six panels of the normalized magnetic vector potential (Ψ) solution proposed in this manuscript, named in (28). Each panel corresponds to a different value of the parameter ν was varied with fixed $a = 1$ values of 1.0, 1.6, 1.8, 2.0, 3.0, and 4.0 in panels a) to f), respectively. The singularity points are located at the points $(0, 0)$, $(\pm 0.48, 0)$, $(\pm 0.53, 0)$, $(\pm 0.58, 0)$, $(\pm 0.71, 0)$, $(\pm 0.77, 0)$, in panels a) to f), respectively. The X-axis ranges from -2 to 2, and the Z-axis ranges from -1 to 1. See details in the text.

any region of the graph; there is a uniform distribution of currents throughout the visualization region.

In panel c), with a higher value of ν, specifically $\nu = 1.8$, the singular points appear further away from the Z-axis, and as a result, the presence of four coexisting magnetic islands becomes evident. This is the first solution in the scientific literature to demonstrate this magnetic morphology. The remaining panels show that as ν increases, the singular points move apart, leading to an increasing confinement of the four islands due to the presence of the external field. In the final panel, the surrounding islands take on a ring-like shape. However, at the center, there is a singularity with an increasingly structured magnetic field around it, resembling the Yoon-Lui 1 solution in the case where $\nu \neq 1$. As ν continues to increase, the ring becomes more structured, i.e., more confined.

The solution presented in the panels of Figure 3 is relevant to Plasma Physics and Space Physics. The observed magnetic islands and singular points in these configurations provide valuable insights into the understanding of magnetic structures in plasmas. These structures play a crucial role in the confinement and stability of plasmas in various contexts, such as controlled nuclear fusion and interactions of solar wind plasma with the Earth's magnetosphere.

In Plasma Physics, the presence of magnetic islands and singular points can impact the dynamics and stability of confined plasma, influencing the design and operation of magnetic fusion devices.

In Space Physics, magnetic islands and singular points are relevant to the study of the magnetosphere and solar wind. These structures play a fundamental role in the acceleration of charged particles and energy transport in magnetized regions of space.

Therefore, the solution presented in the panels of Figure 3 contributes to the understanding of these plasma phenomena in different scientific contexts and

 DOI: https://doi.org/10.1590/1806-9126-RBEF-2023-0217

can be explored in the development of theoretical models and interpretation of experimental observations, driving advancements in Plasma Physics and Space Physics.

In the continuation of this series, in part 3, we will delve further into the study and understanding of the Grad-Shafranov equation. This next stage will focus on exploring the synergy between the Yoon-Lui-2 and Yoon-Lui-3 generator functions [31, Sections 8 and 9]. It presents an exceptional opportunity to gain valuable insights into the behavior of plasma in magnetic confinement systems and geospatial environments. Do not miss out on this chance to expand your knowledge. Keep reading and immerse yourself in all that part 3 has to offer!

6. Conclusion

In conclusion, this study presents a significant breakthrough by introducing a novel solution for the magnetic field in confined plasma systems. By combining the generating functions of the Yoon-Lui-1 and Yoon-Lui-3 models, fresh insights into magnetic structures in plasmas are provided. The derived solution is analyzed using density graphs across various parameter values, revealing singular points that play a crucial role in understanding the solution's behavior. This solution holds great potential for improving plasma confinement efficiency and has applications in Plasma Physics and Space Physics.

Furthermore, this article highlights the importance of understanding magnetic structures in plasmas and their impact on confinement and stability in various contexts. The new solution contributes to theoretical models and the interpretation of experimental observations. It offers valuable knowledge for controlled nuclear fusion and the interaction of solar wind plasma with the Earth's magnetosphere.

Moreover, this article demonstrates the integration of scientific literature into physics education, promoting a deeper understanding of the Grad-Shafranov equation and complex plasma phenomena. By combining existing knowledge and employing mathematical analysis, students are empowered to become innovative thinkers and problem solvers in the field of plasma physics and space physics.

By showcasing the power of combining knowledge and emphasizing the integration of scientific literature, this study equips future physicists with the necessary tools and skills for advancements in understanding magnetic structures and plasma confinement. It fosters a comprehensive understanding of physical concepts, driving advancements and innovations in plasma physics and contributing to a deeper understanding of the universe.

Acknowledgments

A. Ojeda-González would like to thank the Brazilian research agencies CNPq for their financial support (Projects 431396/2018-3 and 302939/2022-9). In addition, thanks to CAPES for the financial support (grants 88881.691438/2022-00 and 88887.709579/2022-00). V. De la Luz thanks CONACYT for their financial support (Basic Science Project with number 254497) and UNAM/PAPIIT TA101920. L. Nunes dos Santos thanks PROSUC-CAPES for the doctoral scholarship in the Physics and Astronomy course at UNIVAP. S. Pilling acknowledges the Brazilian research agencies CNPq (Projects 302985/2018-2 and 302608/2022-2). Project linked to CNPq research group "*Applied Mathematics to Space Physics*".

References

[1] A. Ojeda-Gonzalez, L. Santos, V. De La Luz, M. Cristaldo-Oliveira, A. Laurindo Sousa, A. Prestes, V. Klausner and S. Pilling, Rev. Bras. Ensino Fis. **45**, e20230104 (2023).

[2] G. Ambrosino and R. Albanese, Control Systems IEEE **25**, 76 (2005).

[3] C. Atanasiu, S. Günter, K. Lackner and I. Miron, Physics Of Plasmas **11**, 3510 (2004).

[4] K. Lackner, Computer Physics Communications **12**, 33 (1976).

[5] P.J. Mc Carthy, Phys. Plasmas **6**, 3554 (1999).

[6] H. Hasegawa, H. Zhang, Y. Lin, B. Sonnerup, S. Schwartz, B. Lavraud and Q. Zong, Journal Of Geophysical Research (Space Physics) **117**, eA09214 (2012).

[7] Q. Hu, Science China Earth Sciences **60**, 1466 (2017).

[8] L. Hau and B. Sonnerup, Journal Of Geophysical Research **104**, 6899 (1999).

[9] B. Sonnerup and W. Teh, Journal Of Geophysical Research (Space Physics) **114**, eA04206 (2009).

[10] H. Li, X. Feng, P. Zuo and Y. Xie, Science In China E: Technological Sciences **52**, 2555 (2009).

[11] A. Isavnin, E. Kilpua and H. Koskinen, Sol. Phys. **273**, 205 (2011).

[12] Q. Hu and B. Sonnerup, J. Geophys. Res. **107**, 1142 (2002).

[13] K. Arzner and M. Scholer, J. Geophys. Res. **106**, 3827 (2001).

[14] J. Birn and M. Hesse, J. Geophys. Res. **106**, 3737 (2001).

[15] U. Becker, T. Neukirch and K. Schindler, J. Geophys. Res. **106**, 3811 (2001).

[16] M. Hesse, J. Birn and M. Kuznetsova, J. Geophys. Res. **106**, 3721 (2001).

[17] M. Kuznetsova, M. Hesse and D. Winske, J. Geophys. Res. **106**, 3799 (2001).

[18] A. Otto, J. Geophys. Res. **106**, 3751 (2001).

[19] M. Shay, J. Drake, B. Rogers and R. Denton, J. Geophys. Res. **106**, 3759 (2001).

[20] Y. Ma and H. Zhang, in: *IEEE International Conference on Multimedia and Expo (ICME)* (Tokyo, 2001).

[21] P. Pritchett, J. Geophys. Res. **106**, 3783 (2001).

[22] B.U.Ö. Sonnerup, H. Hasegawa, W.L. Teh and L.N. Hau, Journal Geophys. Res. **111**, A09204 (2006).

[23] A. Ojeda-Gonzalez, V. Klausner, O. Mendes, M.O. Domingues and A. Prestes, Sol. Phys. **292**, 160 (2017).

[24] Q. Hu and B.U. Ö Sonnerup, Geophys. Res. Lett. **28**, 467 (2001).

[25] J.R. Kan, Journal Geophys. Res. **78**, 3773 (1973).

[26] J.R. Kan, Plan. Space Sci. **27**, 351 (1979).

[27] A. Ojeda-Gonzalez, M.O. Domingues, O. Mendes, M.K. Kaibara and A. Prestes, Braz. J. Phys. **45**, 493 (2015).

[28] M. Cristaldo-Oliveira, A. Ojeda-Gonzalez, L.N. Santos, A. Prestes and A.N. Laurindo-Sousa, Rev. Bras. Ensino Fis. **42**, e20200297 (2020).

[29] K. Schindler, *Physics of Space Plasma Activity* (Cambridge University Press, Cambridge, 2006).

[30] G.W. Walker, Proc. R. Soc. Lond. A. **91**, 410 (1915).

[31] P.H. Yoon and A.T.Y. Lui, Journal Geophys. Res. **110**, A01202 (2005).

[32] V. Génot, JGR Space Phys. **110**, A09214, (2005).

[33] M. Scholer, Geophysical Research Letters **15**, 291 (1988).

[34] E. Priest and T. Forbes, Journal Of Geophysical Research: Space Physics **97**, 1521 (1992).

[35] M. Bussac, R. Pellat, J. Soule and M. Tagger, Physics Letters A **105**, 51 (1984).

[36] J. Guo, S. Lu, Q. Lu, Y. Lin, X. Wang, K. Huang, R. Wang and S. Wang, Journal Of Geophysical Research: Space Physics **126**, e2020JA028670 (2021).

[37] A. Sousa, A. Ojeda-Gonzalez, A. Prestes, V. Klausner and L.A. Caritá, Brazilian Journal Of Physics **48**, 67 (2018).